# Fibre Distribution and the Process-Property Dilemma

**John Summerscales**
Advanced Composites Manufacturing Centre, School of Marine Science and Engineering,
Plymouth University, Drake Circus, Plymouth, PL4 8AA, United Kingdom.
E: jsummerscales@plymouth.ac.uk T: +44 1752 586150

**Abstract**
The options for the fibre reinforcement of polymer matrix composites cover a range from short-fibre chopped strand mat, through woven fabric to unidirectional pre-impregnated (prepreg) reinforcements. The modelling of such materials may be simplified by assumptions such as perfect regular packing of fibres and the total absence of fibre waviness. However, these and other features such as the crimp or waviness in woven fabrics make real materials more complex than the simplified models. Clustering of fibres creates fibre-rich and resin-rich volumes (FRV and RRV respectively) in the composites. Prior to impregnation, large RRV will be pore-space that can expedite the flow of resin in liquid composite moulding processes (especially resin transfer moulding (RTM) and resin infusion under flexible tooling (RIFT). In the composite, the clustering of fibres tends to reduce the mechanical properties. The use of image processing and analysis can permit micro-/meso-structural characterisation which may correlate to the respective properties. This chapter considers the quantification of microstructure images in the context of the process-property dilemma for woven carbon-fibre reinforced composites with the aim of increasing understanding of the balance between processability and mechanical performance (185 words).

**Keywords:** fibre distribution, fractal dimension; process-property relationships; tessellation

## 1 Introduction

For high-performance continuous fibre-reinforced (advanced) composites, as the fibre volume fraction increases, (a) the reduction of the pore-space, and hence permeability of the reinforcement, makes long-range flow processes such as liquid composite moulding slower, and (b) the mechanical properties increase. For real engineering structures, it is essential to balance this process-property dilemma by appropriate choice of the micro-/meso-structural features of the reinforcement architecture. This chapter will review research which aims to understand the inter-relationships between the factors above.

### *1.1 Process*

There are a variety of liquid moulding technologies, known as Liquid Composite Moulding (LCM), for the manufacture of fibre-reinforced composites. LCM (Rudd et al, 1997) includes Resin Transfer Moulding (RTM) (Potter, 1997. Kruckenberg and Paton, 1998. Parnas, 2000), where the flow of the resin may occur principally in the plane of the reinforcement, and Resin Infusion under Flexible Tooling (RIFT) (Williams et al 1996, Cripps et al, 2000. Summerscales and Searle, 2006. Summerscales, 2012) where the flow processes may occur in all three dimensions.

Darcy's law (Darcy, 1856), originally derived to model the flow of water in the Dijon aquifers, has been adopted to model LCM flow processes by the inclusion of a viscosity term. Equation 1 is for the isotropic case, although the anisotropy within composites normally requires the tensor relationships:

$$\mathbf{Q = k\ A\ \Delta P\ /\ \mu\ L} \qquad \mathbf{(1)}$$

where Q is the volumetric flow rate ($m^3/s$), K is a constant of proportionality known as the permeability ($m^2$), A is the cross section of the porous medium normal to the flow direction ($m^2$), $\Delta P/L$ is the pressure gradient driving the flow (Pa/m) and $\mu$ is the fluid viscosity (Pa.s). However, the original model was for fully saturated flow and LCM is an unsaturated flow process. The recent round-robin tests (Arbter et al, 2011. Vernet et al, 2014) aimed to develop a standard permeability test using saturated flow with model fluids. Cogswell (1988) has stated "It is clear that in the study of permeability of composite materials, an issue [the potential significance of surface tension effects] so critical to the quality of the finished product, we cannot rely simply on D'Arcy's law. What is needed to replace this is unclear, but considerable effort is being directed to resolving this matter". Summerscales (2004) reviewed the literature which indicates that absolute permeability values may be dependent on the choice of permeant, further reinforcing the need to understand the interfacial surface tensions. Model fluids could still be useful for ranking the relative permeabilities of different reinforcements.

The permeability, K, can be predicted using the Kozeny-Carman (Kozeny, 1927. Carman, 1937) Equation (2):

$$\mathbf{Q = \varepsilon A m^2 \Delta P / k \mu L} \quad \textbf{(2)}$$

where ε is the porosity ($1-V_f$), $V_f$ is the fibre volume fraction, m is the *mean* hydraulic radius, and k is the Kozeny constant.

Blake (1922) defined the hydraulic radius, m (Equation 3), as the volume in which fluid actually flows, εV (where V = AL), divided by the wetted surface area (S):

$$\mathbf{m = \varepsilon.V/S} \quad \textbf{(3)}$$

$$\mathbf{\therefore Q = \varepsilon^3.A.V^2.\Delta P/k.\mu.S^2.L} \quad \textbf{(4)}$$

Until fibres touch, the increase in surface area (Summerscales, 2000) will be linear with volume fraction ($V_f^2$ is substituted for $S^2$) as in expression (5).

$$\mathbf{\therefore K \propto (1-V_f)^3 / V_f^2 \quad \textit{or} \quad \varepsilon^3 / (1-\varepsilon^2)} \quad \textbf{(5)}$$

Summerscales (1993) showed that as fibres gather into increasingly large clusters with the inter-fibre spaces closed-off from flow, the permeability increases as the wetted area decreases despite the reduction in effective flow area due to the inaccessible inter-fibre volumes.

Wang and Grove (2008) and Wang et al (2009) used a dual-scale resin infusion model to show a characteristic relationship between tow impregnation speed, the macro-scale resin pressure surrounding the tow and the degree of tow saturation. They introduced a sink and a source term into the two different scaled flows (intratow and intertow) to couple them together.

The estimation of the permeability of "real" reinforcements is now a feature of a number of 3-D flow modelling and textile design software packages, e.g. FibreSIM, TexGen and WiseTex (Celper and FlowTex).

### *1.2 Properties*

The principal elastic and strength properties of a fibre reinforced composite material can be estimated/predicted using rules-of-mixture. These equations have recently been extended for natural (and other non-circular cross-section) fibre composites to the forms in Equations (6) and, for unidirectional composites, (7) (Virk et al, 2012):

$$\mathbf{E_c = \kappa \eta_d \eta_l \eta_o V_f E_f + V_m E_m} \quad \textbf{(6)}$$

$$\mathbf{\sigma'_c = \kappa \sigma'_f V_f + \sigma_{m*} V_m} \quad \textbf{(7)}$$

where $E_x$ is the tensile/compressive modulus, $V_x$ is the volume fraction, κ is a fibre area correction factor (FACF) for fibre properties which have been calculated with an (incorrect) assumption of circular cross-section (Virk et al, 2012), $\eta_d$ is a fibre diameter distribution factor (Summerscales et al, 2011), $\eta_l$ is a fibre length distribution factor (Cox, 1952), $\eta_o$ is a fibre orientation distribution factor (Krenchel, 1964), $\sigma'_x$ is a strength, $\sigma_{m*}$ is the stress in the matrix at the failure strain of the fibre and subscripts x are c (composite), f (fibre) and m (matrix) respectively. For continuous circular cross-section fibres, κ, $\eta_d$ and $\eta_l$ all default to 1 so both equations simplify to their standard forms.

### *1.3 Voids and resin-rich volumes*

In Equations (6) and (7), the total volume fraction for a monolithic fibre composite will be given by Equation 8:

$$\mathbf{V_f + V_m + V_v = 1} \quad \textbf{(8)}$$

where subscript v indicates the void content. In an ideal composite before resin impregnation, $V_v$ is the volume available for flow ($\varepsilon = 1-V_f$ with $V_m = 0$). However, few processes produce perfect materials, so porosity (connected pores) and voids (separate bubbles) do occur in composites. The causes may include (i) air in the

resin mix, (ii) volatiles in the resin "boiling", (iii) the degree of impregnation of pre-impregnated materials, (iv) trapping air between prepreg layers, or (v) race-tracking in LCM processes.

Judd and Wright [18], Ghiorse [19] and Baley et al [20] have reviewed porosity/voids in composites. Judd and Wright concluded that "although there is a considerable scatter in results (reflecting in part the difficulties of accurate void content determination) the available data show that the interlaminar shear strength of composites decreases by about 7 per cent for each 1 per cent voids up to at least the 4 per cent void content level, beyond which the rate of decrease diminishes. Other mechanical properties may be affected to a similar extent. This is true for all composites regardless of the resin, fibre or fibre surface treatment used in their fabrication". See Table 1 of Judd and Wright for a comprehensive analysis of the data. It may be time to consider whether the above findings remain relevant to modern toughened resin systems.

Stone and Clarke (1975) reported that (a) below $V_v$ = 1.5%, voids tend to be volatile-induced and hence spherical with diameters in the range 5-20 μm, while (b) above $V_v$ = 1.5%, the voids are flattened and elongated in the in-plane direction due to the limitation of space between the fibre bundles and are also significantly larger than those voids at a lower $V_v$. Mayr et al (2011) reported that small pores in CFRP with porosity levels <1.8% often have roughly circular cross-sections and found an abrupt increase in the out-of-plane shape factors at this percentage porosity.

Purslow (1984) proposed a novel classification system for voids and considered the earlier system was only significant for fairly uniformly distributed voids. For example, to quote a $V_v$ of 0.5% for a composite of generally high quality (voids < 0.2%) but with an occasional very large void could be very misleading and potentially dangerous. It is difficult to measure void contents to such low values. He suggested that the void content should be quoted as "0<voids<0.2%; infrequent local voids > 0.5%". His studies have suggested that when $V_v$ < 0.5%, the voids are spherical with a diameter of 10 μm and are due to trapped volatiles. As $V_v$ increases, the voids due to trapped volatiles decrease in number and are replaced by large intra-tow/intra-lamina voids. The results suggested a linear relationship between $V_v$ and void thickness, where the thickness is related to fibre diameter.

Alhuthali and Low (2013) reported densities, fibre volume fractions and void contents for recycled cellulose fibres (RCF: density 1540 kg/m$^3$) in vinyl-ester resin (VER: density 1140 kg/m$^3$) (Table 1). As fibre weight fraction increased, the theoretical and experimental composite densities rose, but there was a clear reduction in void content at a greater rate than predicted from the reduced matrix volume fraction (column 7 of the Table).

**Table 1: Fibre volume fraction and void content of RCF/VER composites**
(extended from Alhuthali and Low (2013) data)

| Sample | Fibres weight fraction | Fibre volume fraction | Theoretical density (kg/m$^3$) | Experimental density (kg/m$^3$) | Void content (%) | [By JS] %void in resin |
|---|---|---|---|---|---|---|
| **20% RCF/VER** | 0.2 | 0.16 | 1210 | 1180±30 | 5.55 | 6.61% |
| **30% RCF/VER** | 0.3 | 0.24 | 1240 | 1210± 20 | 4.75 | 6.25% |
| **40% RCF/VER** | 0.4 | 0.33 | 1270 | 1240± 50 | 3.28 | 4.89% |
| **50% RCF/VER** | 0.5 | 0.43 | 1310 | 1270± 20 | 2.74 | 4.81% |

Close (2009) has published an interesting account of what remains when you take all the matter away.

### *1.4 Micro-/meso-structural characterisation*

The use of microscopy to reveal fine detail in structures has a long history (Allen, 2015). The distribution of features within a plane or volume may be quantified in a variety of ways. The classification of structured populations can be achieved using a variety of parameters, e.g. (a) nearest-neighbour index (Clark and Evans (1954), (b) chi-squared analysis (Davis, 1974), (c) quadrat analysis (Greig-Smith, 1952), mean free path and mean random spacing (Cribb, 1978), space auto-correlograms (Mirza, 1970), area fraction variance analysis and mean intercept length (Li, 1992) and contiguity index (Short and Summerscales, 1984). In recent years, the quantification of microstructures has been achieved using tessellation techniques or, latterly, fractal dimensions which are reviewed in the following sections.

The nature of fibre-reinforced composites is such that there is generally dual-scale structure with clustering of fibres in bundles (tows) and larger features dictated by the reinforcement architecture (e.g. chopped strand mat, woven fabrics or stitched non-crimp fabrics (NCF)). The microstructure of fibre-reinforced composites is

normally defined using the parameters in Equation (6). This data may be insufficient where clustering of fibres occurs. The use of image processing and analysis for the characterisation of composite micro-/meso-structures has been the subject of a number of publications (e.g. Guild and Summerscales, 1993. Pyrz, 2000a/b. Summerscales, 1998. Summerscales et al, 2001).

The morphological description of the dispersion of phases at the micro-/meso-structural level is an important factor for the determination of the overall behaviour of the macro-composites. The micro-failure threshold is dominated by fluctuations in the local stress field. These "hot spots" are a function of the local disorder of the reinforcement (Pyrz, 2000a).

## 2 Tessellation techniques

The analysis of a plane with a number of non-overlapping objects (e.g. fibre cross-sections in a micrograph), can be achieved by identifying the centroid of each object and using that set of points. The Delaunay (1934) tessellation simply joins adjacent points to produce a series of contiguous triangles where no point is inside the circumcircle of any triangle. The Voronoi diagram (also known as the Dirichlet tessellation, which is the complement (dual) of the Delaunay tessellation) partitions the plane into convex polygons where each polygon contains just one generating point and every point in each individual polygon is closer to its own generating point than to any of the other points. The cells are called Dirichlet regions, Thiessen polytopes, or Voronoi polygons (Dirichlet, 1850, Voronoi, 1907. Weisstein, 2015). For each Delauney tessellation, there will be a unique Voronoi diagram, and *vice versa* (Figure 1). The lines between the generating points in the Delaunay tessellation will be orthogonal to the edge of the Voronoi polygons (Ringler, 2008).

Summerscales et al (1993) studied unidirectional carbon-fibre reinforced epoxy composites manufactured using vacuum-bag processing with different "dwell-times" before pressure was applied to consolidate the laminates. The cross-section microstructure was described using the size of the Voronoi cell around each fibre and found to be dependent on the manufacturing parameters. Samples with a 90-minute (rather than 0- or 180- minute) dwell time were found to have the lowest thickness (highest fibre volume fraction) and to be the least clustered (i.e. the most uniform fibre distribution). The plate was believed to be processed within the optimum viscosity limits (7500-16500 mPa.s) identified by Stringer (1989).

Griffin et al (1995a) conducted permeability experiments on a series of five 2x2 twill weave carbon fibre fabrics containing a variable number of twisted/bound flow-enhancing tows (FET) in the weft direction. The permeability was found to be dependent on the flow fluid used, but values for a single fluid showed the expected increase in permeability with number of FET. Quantitative microscopy revealed that flow enhancement was accompanied by the presence of large flow areas adjacent to the FET and increased in line with the average perimeter of these areas. The transverse section composite microstructure was characterised using maximum feature height and width (vertical and horizontal ferets, i.e. the two orthogonal pairs of parallel tangents on the outer boundaries of a feature), x- and y- centres of gravity and perimeter. The recorded perimeters were broadly aligned with the expectation of the Blake-Kozeny-Carman equations (Equations 2-4) although it was not practical to determine the effective penetration of the flow front into the tows during wetting. Griffin et al (1995b) used three of the above reinforcements to measure the total number of areas, and values of total area, for the three laminates (Table 2) and used the zones of influence (Voronoi cells) to compare fibre separations within either the normal tows ($V_f$ =40%) or the FET ($V_f$ = 57%) in the orthogonal horizontal/vertical directions.

**Table 2 Pore areas and for the 2x2 twill weave laminates**

| Fabric/ Laminate | % FET | Number of flow areas | Total area of pore space ($mm^2$) | Normalised flow rate (centipoise mm/s) (*sic*) |
|---|---|---|---|---|
| Twill | 0.0 | 210 | 5.47 | 796 |
| 156 | 12.5 | 115 | 8.54 | 5200 |
| 126 | 50.0 | 310 | 11.21 | 7982 |

Summerscales et al (1995) used a radial flow permeameter to measure the permeabilities of the above five fabrics and found increasing permeability with increasing number of FET (Table 3). Basford et al (1995) measured the mechanical properties of laminates manufactured with these fabrics and found that both compression and apparent interlaminar shear strengths (ILSS) decreased with increasing proportion of FET (Table 3).

Everett (1996) used Radial Distribution Functions (RDF) to describe composite material microstructures and reported that the proximity of near-neighbours has important ramifications for the micromechanical modelling

of tow-based composites. Bertoncelj et al (2016).used the RDF approach in conjunction with Voronoi diagrams to quantify random fibre arrangements.

The use of tessellation normally produces data as histograms. Selection of specific sub-sets of that data may correlate to measured material parameters, but the choice of sub-set is normally subjective.

**Table 3: Reinforcement fabric construction, microscopical parameters, permeabilities and mechanical properties.**

| Fabric/ laminate | % FET | Total perimeter (mm) | Total area ($mm^2$) | Permeability (darcies) | Compression strength (MPa) | ILSS (MPa) |
|---|---|---|---|---|---|---|
| 38166 (twill) | 0.0 | 12.7 | 0.38 | 36 | 245 | 49.9 |
| 156 | 12.5 | 12.5 | 0.49 | 259 | 218 | 44.0 |
| 150 | 16.7 | 12.8 | 0.50 | 306 | 201 | 43.0 |
| 148 | 25.0 | 18.0 | 0.91 | 389 | 173 | 44.6 |
| 126 | 50.0 | 22.1 | 1.24 | 291 | 128 | 30.5 |

## 3 Fractal dimensions

In conventional notation, a point has dimension 0, a line has dimension 1, an area has dimension 2 and a volume has dimension 3. If a square is decomposed into four ($2 \times 2 = 2^2$) self-similar smaller squares it has magnification 2, and if decomposed into nine ($3 \times 3 = 3^2$) smaller squares it has magnification 3. The dimension is simply the exponent of the number of self-similar pieces with into which the figure has been decomposed (Devaney, 1995). The total number of objects, N, is a function of the magnification factor, r, and the dimension, D as given by $N = r^D$.

In Euclidean geometry the exponent will be an integer, but in fractal geometry it can be a real number. Fractal geometry is the complement of Euclidean geometry and crystal symmetry (Pyrz, 2000a). Richardson (1961 posthumous publication) pioneered a process for calculating the length of a coastline using rulers of varying lengths which was popularised as fractal geometry by Mandelbrot (1967, 1982).

The fractal dimension, FD, measures the complexity of a self-similar object. The box-counting method (BCM) extends the perimeter measuring method used for coastlines by covering the image with a grid. The number of elements of the grid which cover features within the image are counted. As increasingly fine grids (smaller boxes) are used, the structure of the pattern is more accurately captured, but now N is the number of boxes that cover the features (Figure 2). The BCM has been widely used in fractal dimension research (Foroutan-Pour et al, 1999. Pitchumani and Ramakrishnan, 1999. Lopes and Betrouni, 2009. Mishnaevsky, 2011).

The slope of the Richardson plot (measured length plotted against the size of the measure, *or*, for the box-counting method, detected area plotted against box size with both plots on a log-log scale) gives the fractal dimension. The definition of the fractal dimension (FD) for a self-similar object is given by Equation 9:

$$\mathbf{FD = \log (N) / \log (r)} \qquad \mathbf{(9)}$$

Both the Richardson plot and BCM appear to be applicable for patterns with or without self-similarity (Borges and Peleg, 1996. Damrau et al, 1997. Foroutan-Pour et al, 1999. Pitchumani and Ramakrishnan, 1999).

### *3.1 Discontinuous fibre composites*

Worrall and Wells (1996) used fractal variance analysis to characterise differences in filamentisation (i.e. fibre separation) between bundled and filamentised press-moulded long discontinuous glass-fibre/polyester resin composites. Changes in the Richardson plot were used to identify changes in the optical micrographs of composite structures.

### *3.2 Continuous fibre composites*

Dzenis et al (1994) used an atomic force microscope to analyse the "self-affinity" of surface topography for several reinforcement fibres. The fractal dimensions of the surfaces were determined as 2.09 ("graphite"), 2.37 (Kevlar®149), 2.52 (undrawn polyimide) and 2.18 (polyimide with a draw ratio of 8). Dzenis (1997) then defined the interfacial fractal dimension as smooth interface (2.0), moderate irregularity (2.4) and very strong irregularity (2.8). He further presented analytical formulations for a variety of elastic, visco-elastic and thermal properties of unidirectional composites in both the axial and transverse directions.

Pearce et al (1998a) investigated the effects of fabric architecture on the processing and properties of 6K carbon fibre reinforced composites using three different weave styles with the same areal weight (290 gsm) and woven from the same batch of fibre. Composites were produced by resin transfer moulding in an unsaturated radial flow permeameter using 9 ($V_f$ = 49%), 10 ($V_f$ = 54%) or 11 ($V_f$ = 60%) layers. Pore space was determined from transverse sections. Interlaminar shear strength was measured in accordance with CRAG Standard Method 100 (Curtis, 1988). The permeabilities for the three fabrics were ranked in the same sequence as the proportion of larger pore spaces (>0.5 $mm^2$), and ranked in the same order as descending ILSS (Table 4).

**Table 4: Carbon fibre fabrics studied**

| Designation | Weave description | No.pore space areas | Average pore space ($mm^2$) | Maximum pore space ($mm^2$) | Permeability range ($x10^{-12}$ $m^2$) | Relative ILSS |
|---|---|---|---|---|---|---|
| E3853 G986 | 2 x 2 twill | 1445 | 0.053 | 1.007 | 34.0-53.7 | lowest |
| E3833 G963 | 5-harness satin Injectex | 2061 | 0.056 | 0.705 | 18.9-36.1 | middle |
| E3795 | 5-harness satin | 2498 | 0.027 | 0.319 | 8.1-17.9 | highest |

In further work on the same fabrics, Pearce et al (1995b) added tensile and compressive tests and fractal analysis of transverse sections to obtain fractal dimensions for the three fabrics. Variations in permeabilities and mechanical properties were related to observed differences in the microstructure. The ranking of ILSS and both tensile and compressive moduli was satin> twill>Injectex. For both the tensile and compressive ultimate strengths, the satin fabric again had the highest properties, with twill generally having marginally better properties than the Injectex. The compressive strengths were lower (around one-half) than the respective tensile strengths for all fabrics as expected due to the pre-buckling of fibres arising from the crimp of the fabrics. Table 5 shows the relative magnitudes of the respective properties and the fractal dimension for each type of fabric.

**Table 5: Summary Pearce et al (1995b) results for all tests showing ranking of fabrics**

| Property | Ranking | | | | |
|---|---|---|---|---|---|
| Permeability | satin | < | Injectex | < | twill |
| Apparent ILSS | satin | > | Injectex | > | twill |
| Tensile modulus | satin | > | twill | > | Injectex |
| Tensile strength | satin | > | twill | > | Injectex |
| Compressive modulus | satin | > | twill | > | Injectex |
| Compressive strength | satin | > | twill | > | Injectex |
| Fractal dimension | satin | > | twill | > | Injectex |

Pearce et al (2000) sought to correlate variations in permeability, and in the laminate mechanical properties, to differences in microstructure using a series of experimental carbon fibre fabrics woven to incorporate a novel flow enhancement concept (use of different proportions of 3K weft tows in a 6K fabric). Permeability data was derived from measurements made during manufacture of the composite plates in a transparent radial flow RTM mould. The manufactured plates were subsequently sectioned for mechanical testing (moduli and strengths in tension and compression) and for automated image analysis to determine fractal dimensions from polished sections. The increase in permeability was not consistent with the proportion of flow-enhancing (3K) tows, but could be ranked in the same sequence as the fractal dimension derived from polished sections (Figure 3). Note that the software used to generate the data returns FD values reduced by one. The compression strengths were unaffected by the change in tow size. The weft direction had lower moduli in both tension and compression. The rate at which modulus decreases with increasing proportion of 3K tows was broadly consistent with the change in volume fraction of fibres in the test direction. The weft tensile strength was ranked in the same sequence as the fractal dimension (Figure 4).

Using the single average data set in Figure 4, we might speculate that extrapolation of the weft tensile strength Excel Trendline to integer values could yield important information. At FD = 0, the intercept at 97 MPa is of a similar magnitude to that expected by extrapolation of the cast resin tensile strengths for the Ampreg 26 epoxy/26SL slow hardener system (the Gurit Ampreg 26 Epoxy laminating system manufacturers data sheet PDS-Ampreg 26-12-0515 gives room temperature cure 58 MPa, 50ºC post-cure 80.3 MPa, 80ºC post-cure (as used) strength not given. At FD =1, the prediction of 1540 MPa is of the order of the strength of a carbon fibre that has been through textile processes (the original paper/thesis that provided the data does not specify the specific grade of fibre used). Subsequent work by different researchers has not reproduced the above finding.

Summerscales et al (2004) quantified 150 X-ray CT cross-sectional slices of plain woven E-glass fibre-reinforced epoxy resin using fractal dimension. The analysis returned a consistent numerical value for each of the slices in the two similar orthogonal planes.

Aniszewska and Rybaczuk (2009) presented simulated quasi-static fracture processes for parallel fibre reinforced composites using cellular automata and BCM fractal characteristics of defects growth. Defect evolution in composites was treated as a dynamical system depending on external and internal conditions and properties of fibres. The simulations were intended to inform further work on the evolution of fractal characteristics for 3D textile-reinforced aluminium matrix composites.

Pimenta and Pinho (2014) have presented a model for the translaminar tensile toughness of fibre-reinforced polymer matrix composites. The model is based on fibre and interfacial properties and assumes a hierarchical failure process with the formation of stochastic variations of quasi-fractal fracture surfaces. The model could reproduce the effect of different types of fibre and matrix, and revealed a marked increase in toughness for thicker plies.

## 4 Concluding remarks

There is increasing evidence that the distribution of fibres within a composite has important effects on the properties, especially the permeability and strengths. In general, the permeability in LCM processes increases with fibre clustering but the consequent resin-rich volumes depress composite strengths. A variety of techniques have been employed to describe micro-/meso-structural fibre (or the complementary resin-rich volume) distributions. Tessellation techniques have dominated this analysis in recent decades. The use of fractal dimension (FD) is becoming increasingly widespread.

The majority of sampling of composite microstructures to date has used (sequential) 2-D sections of the material. Confocal laser scanning microscopy (CSLM) (Shotton, 1989. Ferrando and Spiess, 2000) within the limits of depth of light penetration, and x-ray computed tomography (XCT) (Miller et al, 2007. Helliwell et al, 2013. Maire and Withers, 2014) could extend this analysis to 3-D sampling. However, the 3-D analysis will incur increased complexity and require more computational time.

## 5 Acknowledgements

The author acknowledges with sincere thanks the collaborations with Professor Felicity Guild as the primary stimulus for his interest in microstructural characterisation. Further acknowledgement is due to Paul Russell who did much of the image analysis in the early studies. The various co-authors of referenced papers were also critical to our achievements in these studies. Finally, I very much appreciate the review by Stephen Grove of a late draft manuscript. Any remaining issues are the responsibility of the chapter author!

## 6 References


- A Alhuthali and I M Low (2013), *Effect of prolonged water absorption on mechanical properties in cellulose fibre reinforced vinyl-ester composites*, Journal of Materials Science, September 2013, **48(18)**, 6331-6340. DOI: 10.1007/s10853-013-7432-4.
- T Allen (2015), Microscopy: A Very Short Introduction, Oxford University Press, Oxford, 2015. ISBN: 978-0-19-870126-2.
- D Aniszewska and M Rybaczuk (2009), Fractal characteristics of defects evolution in parallel fibre reinforced composite in quasi-static process of fracture, Theoretical and Applied Fracture Mechanics, October 2009. **52(2)**, 91-95. DOI: 10.1016/j.tafmec.2009.08.002.
- R Arbter, J M Beraud, C Binetruy, L Bizet, J Bréard, S Comas-Cardona, C Demaria, A Endruweit, P Ermanni, F Gommer, S Hasanovic, P Henrat, F Klunker, B Laine, S Lavanchy, S V Lomov, A Long, V Michaud, G Morren, E Ruiz, H Sol, F Trochu, B Verleye, M. Wietgrefe, W Wu, G Ziegmann (2011), *Experimental determination of the permeability of textiles: A benchmark exercise*, Composites Part A: Applied Science and Manufacturing, September 2011, **42(9)**, 1157–1168. DOI: 10.1016/j.compositesa.2011.04.021.
- C Baley, P Davies and D Cartié (2015), *Porosity in ocean racing yacht composites: a review*, Applied Composite Materials, February 2015, **22(1)**, 13-28. DOI: 10.1007/s10443-014-9393-4.
- D M Basford, P R Griffin, S M Grove and J Summerscales (1995), *Research report: the relationship between mechanical performance and microstructure in composites fabricated with flow-enhancing fabrics*, Composites, September 1995, 26(9), 675-679. DOI: *10.1016/0010-4361(95)98917-A.*
- B Bertoncelj, K Vojisavljević, J Rihtaršič, G Trefalt, M Huskić, E Žagar, B Malič (2016), *A Voronoi-diagram analysis of the microstructures in bulk-molding compounds and its correlation with the mechanical*

*properties*, Express Polymer Letters, [refereed 07-Nov-2015 but not yet published].
- F C Blake (1922), *The resistance of packing to fluid flow*, Transactions of the American Institute of Chemical Engineers 1922, **14**, 415-421.
- A Borges and M Peleg (1996), Determination of the apparent fractal dimension of the force-displacement curves of brittle snacks by four different algorithms, Journal of Texture Studies, July 1996, 27(3), 243–255. DOI: 10.1111/j.1745-4603.1996.tb00073.x
- P C Carman (1937), *Fluid flow through a granular bed*, Transactions of the Institute of Chemical Engineers (London), 1937, **15**, 150-166.
- P J Clark and F C Evans (1954), *Distance to the nearest neighbor as a measure of spatial relationships in populations*, Ecology, October 1954, **35(4)**, 445-453. DOI: 10.2307/1931034.
- F Close (2009), Nothing: A Very Short Introduction, Oxford University Press, Oxford, 2009. ISBN 978-0-19-922586-6.
- FN Cogswell, Flow Processes in Composite Materials, Advanced Composites Bulletin, July 1988, 1(10), 1-5.
- H L Cox (1952), *The elasticity and strength of paper and other fibrous materials*, British Journal of Applied Physics, 1952, **3(3)**, 72-79. DOI: 10.1088/0508-3443/3/3/302.
- W R Cribb (1978), *Quantitative metallography of polyphase microstructures*, Scripta Metallurgica, October 1978, **12(10)**, 893-898. DOI: 10.1016/0036-9748(78)90177-1.
- D Cripps, T J Searle and J Summerscales (2000), Open Mould Techniques for Thermoset Composites, In R Talreja and J-A Månson (editors): Comprehensive Composite Materials Encyclopædia, volume 2: Polymer Matrix Composites, Elsevier Science, Oxford, July 2000, Chapter 21, pp 737-761. ISBN 0-08-043725-7. DOI: 10.1016/B0-08-042993-9/00188-1
- P T Curtis (1988), CRAG test methods for the measurement of the engineering properties of fibre reinforced plastics, Royal Aerospace Establishment Technical Report 88 012, February 1988.
- E Damrau, MD Normand and M Peleg (1997), Effect of resolution on the apparent fractal dimension of jagged force-displacement relationships and other irregular signatures, Journal of Food Engineering, February 1997, 31(2), 171–184. DOI: 10.1016/S0260-8774(96)00063-5.
- H P G Darcy (1856), Les fontaines publiques de la ville de Dijon, Dalmont, Paris, 1856.
- P Davis, Describing point patterns, in Science in Geography Book 3: Data Description and Presentation, Oxford University Press, Oxford, 1974, 29-35. ISBN 978-0-19-913067-2.
- B Delaunay (1934), *Sur la sphère vide. A la mémoire de Georges Voronoï*, Bulletin de l'Académie des Sciences de l'URSS. Classe des sciences mathématiques et naturelles, 1934, (6), 793–800.
- R L Devaney (1995), Fractal Dimension, http://math.bu.edu/DYSYS/chaos-game/node6.html, 02 April 1995, accessed 07 November 2015.
- G L Dirichlet (1850), *Über die Reduktion der positiven quadratischen Formen mit drei unbestimmten ganzen Zahlen*, Journal für die reine und angewandte Mathematik, 1850, **40**, 209-227. DOI: 10.1515/crll.1850.40.209.
- Yu A Dzenis, D H Reneker, V V Tsukruk and R Patil, Fractal analysis of surfaces of advanced reinforcing fibers by atomic force microscopy, Composite Interfaces, 1994, 2(4), 307-319. DOI: 10.1163/156855494X00157.
- Yu A. Dzenis, Effective thermo-viscoelastic properties of fibrous composites with fractal interfaces and an interphase, Composites Science and Technology, 1997, 57(8), 1057–1063. DOI:: 10.1016/S0266-3538(96)00171-6.
- R K Everett (1996), *Quantification of random fiber arrangements using a radial distribution function approach*, Journal of Composite Materials, April 1996, **30(6)**, 748-758. DOI: 10.1177/002199839603000606.
- M Ferrando and W E L Spiess (2000), Review: Confocal scanning laser microscopy. A powerful tool in food science, Food Science and Technology International, August 2000, 6(4), 267-284. DOI: 10.1177/108201320000600402
- K Foroutan-Pour, P Dutilleul and D Smith (1999), *Advances in the implementation of the box-counting method of fractal dimension estimation*, Applied Mathematics and Computation, Nov-Dec 1999, **105(2-3)**, 195-210. DOI: 10.1016/S0096-3003(98)10096-6.
- S R Ghiorse (1993), *Effect of void content on the mechanical properties of carbon/epoxy laminates*, SAMPE Quarterly, January 1993, **24(2)**, 54-59.
- P Greig-Smith (1952), *The use of random and contiguous quadrats in the study of the structure of plant communities*, Annals of Botany, April 1952, **NS16(2)**, 293-316.
- P R Griffin, S M Grove, P Russell, D Short, J Summerscales, FJ Guild and E Taylor (1995a) *The effect of reinforcement architecture on the long range flow in fibrous reinforcements* Composites Manufacturing, September-December 1995, 6(3/4), 221-228. DOI: 10.1016/0956-7143(95)95015-Q.

- P R Griffin, S M Grove, F J Guild, P Russell and J Summerscales (1995b), *The effect of microstructure on flow promotion in resin transfer moulding reinforcement fabrics*, Journal of Microscopy, March 1995, 177(3), 207-217. DOI: 10.1111/j.1365-2818.1995.tb03552.x.
- F J Guild and J Summerscales (1993), *Microstructural image analysis applied to fibre composite materials: a review*, Composites, 1993, **24(5)**, 383-394. DOI: 10.1016/0010-4361(93)90246-5.
- J R Helliwell, C J Sturrock, K M Grayling, S R Tracy, R J Flavel, I M Young, W R Whalley and S J Mooney (2013), Applications of X-ray computed tomography for examining biophysical interactions and structural development in soil systems: a review, European Journal of Soil Science, June 2013, 64(3), 279–297. DOI: 10.1111/ejss.12028.
- N C W Judd and W W Wright (1978), *Voids and their effects on the mechanical properties of composites - an appraisal*, SAMPE Journal, January/February 1978, 14(1), 10-14.
- J Kozeny (1927), *Uber die kapillare Leitung des Wassers in Boden*, Sitzungsberichte Akademie der Wissenschaft Wien Math-naturw, 1927, **139(Kl.abt.IIa)**, 271-306.
- H Krenchel (1964), Fibre Reinforcement, Akademisk Forlag, Copenhagen, 1964.
- T M Kruckenberg and R Paton (1998), Resin Transfer Moulding for Aerospace Structures, Kluwer Academic Publishers, Dordrecht NL, 1998. ISBN 0-412-73150-9.
- Q F Li, R Smith and D G McCartney (1992), *Quantitative evaluation of fiber distributions in a continuously reinforced aluminium alloy using automatic image analysis*, Materials Characterization, 1992, **28(4)**, 189-203. DOI: 10.1016/1044-5803(92)90081-R.
- R Lopes and N Betrouni (2009), Fractal and multifractal analysis: a review, Medical Image Analysis, August 2009, 13(4), 634–649. DOI: 10.1016/j.media.2009.05.003
- E Maire and P J Withers (2014), Quantitative X-ray tomography, International materials reviews, January 2014, 59(1), 1-43. DOI: 10.1179/1743280413Y.0000000023.
- BB Mandelbrot (1967), How long is the coast of Britain? Statistical self-similarity and fractional dimension, Science, 5 May 1967, 156(3775), 636-8. DOI: 10.1126/science.156.3775.636.
- BB Mandelbrot (1982), The Fractal Geometry of Nature, W H Freeman & Co, New York, 1982. ISBN 0-7167-1186-9.
- J D Miller, C L Lin and A B Cortes (2007), A review of x-ray computed tomography and its applications in mineral processing, Mineral Processing and Extractive Metallurgy Review, April 2007, 7(1), 1-18. DOI: 10.1080/08827509008952663
- F S M A Mirza (1970), A statistical study of the structure of mixtures in particulate solids, PhD thesis, University of Exeter, 1970.
- L Mishnaevsky (2011), *Hierarchical composites: analysis of damage evolution based on fiber bundle model*, Composites Science and Technology, 2011, **71**, 450-460. DOI: 10.1016/j.compscitech.2010.12.017
- R S Parnas (2000), Liquid Composite Moulding, Hanser Gardner Publications, 2000. ISBN 1-569-90287-9.
- N R L Pearce, F J Guild and J Summerscales (1998a), *An investigation into the effects of fabric architecture on the processing and properties of fibre reinforced composites produced by resin transfer moulding*, Composites Part A: Applied Science and Manufacturing, 1998, 29A(1/2), 19-27. DOI: 10.1016/S1359-835X(97)00028-6
- N R L Pearce, J Summerscales and F J Guild (1998b), The use of automated image analysis for the investigation of fabric architecture on the processing and properties of fibre reinforced composites produced by RTM, Composites Part A: Applied Science and Manufacturing, 1998, 29A(7), 829-837. DOI: 10.1016/S1359-835X(98)00065-7.
- N R L Pearce, J Summerscales and F J Guild (2000), Improving the resin transfer moulding process for fabric-reinforced composites by modification of the fibre architecture, Composites Part A: Applied Science and Manufacturing, 2000, 31A(12), 1433-1441. DOI: 10.1016/S1359-835X(00)00140-8.
- S Pimenta and S T Pinho (2014), *An analytical model for the translaminar fracture toughness of fibre composites with stochastic quasi-fractal fracture surfaces.* Journal of the Mechanics and Physics of Solids, May 2014. **66**, 78-102. DOI: 10.1016/j.jmps.2014.02.001
- R Pitchumani and B Ramakrishnan (1999), *A fractal geometry model for evaluating permeabilities of porous preforms used in liquid composite molding*, International Journal of Heat and Mass Transfer, June 1999, **42 (12),** 2219-2232. DOI: 10.1016/S0017-9310(98)00261-0.
- K Potter (1997), Resin Transfer Moulding, Chapman & Hall, London, 1997. ISBN 0-412-72570-3.
- D Purslow (1984), On the optical assessment of the void content in composite materials, Composites, 1984, 15(3), 207-210. DOI: 10.1016/0010-4361(84)90276-3.
- R Pyrz (2000a), Chapter 1.16: *Morphological characterization of microstructures, in Comprehensive Composite Materials*, Volume 1: Fiber Reinforcements and General Theory of Composites, Elsevier, 2000, pp 465-478. DOI: 10.1016/B0-08-042993-9/00053-X.

- R Pyrz (2000b), Chapter 2.15: *The application of morphological methods to composite materials*, in Comprehensive Composite Materials, Volume 2: Polymer Matrix Composites, Elsevier, 2000, pp 553-576. DOI: 10.1016/B0-08-042993-9/00071-1.
- L F Richardson (1961), *The problem of contiguity: an appendix of statistics of deadly quarrels*, General Systems Yearbook, 1961, 6, 139-187.
- T Ringler (2008), *Introduction to Voronoi diagrams and Delaunay triangulations*, Summer Colloquium on Numerical Techniques for Global Atmospheric Models, National Center for Atmospheric Research (NCAR), Boulder CO, 02-13 June 2008, paper 25. http://www.cgd.ucar.edu/cms/pel/asp2008/25-Ringler-VoronoiDelaunay.pdf, accessed 07 November 2015.
- CD Rudd, AC Long, KN Kendall and CGE Mangin (1997), Liquid Moulding Technologies, Woodhead Publishing, Cambridge, 1997. ISBN 1-85573-242-4.
- D Short and J Summerscales, The definition of microstructures in hybrid reinforced plastics, 5th International Conference of the European Chapter of SAMPE, Montreux ~ Switzerland, 12-14 June 1984, volume 2, paper 19.
- D M Shotton (1989), Confocal scanning optical microscopy and its applications for biological specimens, Journal of Cell Science, 1989, 94, 175-206.
- DEW Stone and B Clarke (1975), *Ultrasonic attenuation as a measure of void content in carbon-fibre reinforced plastics*, Non-Destructive Testing, 1975, **8(3)**, 137-145. DOI: 10.1016/0029-1021(75)90023-7.
- LG Stringer (1989), Optimization of the wet lay-up/vacuum bag process for the fabrication of carbon fibre epoxy composites with high fibre fraction and low void content, Composites, 1989, 20(5), 441-452. DOI: 10.1016/0010-4361(89)90213-9.
- J Summerscales (1993), *A model for the effect of fibre clustering on the flow rate in resin transfer moulding*, Composites Manufacturing, **4(1)**, 27-31 , DOI: 10.1016/0956-7143(93)90013-X
- J Summerscales (editor) (1998), *Microstructural Characterisation of Fibre-Reinforced Composites*, Woodhead Publishing, Cambridge, July 1998. ISBN 1-85573-240-8. DOI: 10.1533/9781855737563.
- J Summerscales (2000), *Appendix B: Fabric permeability*, in D Cripps, TJ Searle and J Summerscales, Chapter 21: Open Mould Techniques for Thermoset Composites, in R Talreja and J-A Månson (editors): Comprehensive Composite Materials, volume 2: Polymer Matrix Composites, Elsevier Science, Oxford, July 2000, pp 737-761. Set ISBN: 0-08-043720-6. DOI: 10.1016/B0-08-042993-9/00188-1.
- J Summerscales (2004), *The effect of permeant on the measured permeability of reinforcement*, 7th International Conference on Flow Processes in Composite Materials (FPCM-7), Newark DE, 7-9 July 2004, 471-476. https://www.fose1.plymouth.ac.uk/sme/fpcm/fpcm07/Extended_abstracts/EA471.pdf
- J Summerscales (2012), Resin Infusion Under Flexible Tooling (RIFT). Encyclopedia of Composites – second edition, John Wiley & Sons, 2012, 2648-2658. DOI: 10.1002/9781118097298.weoc216
- J Summerscales and T J Searle (2005), Review: Low pressure (vacuum infusion) techniques for moulding large composite structures, Proc IMechE Part L: Journal of Materials: Design and Applications, February 2005, L219(1), 45-58. DOI: 10.1243/146442005X10238
- J Summerscales, D Green and F J Guild (1993), *Effect of processing dwell-time on the microstructure of a fibre reinforced composite*, Journal of Microscopy, February 1993, 169(2), 173-182. DOI: 10.1111/j.1365-2818.1993.tb03292.x.
- J Summerscales, P R Griffin, S M Grove and F J Guild (1995), *Quantitative microstructural examination of RTM fabrics designed for enhanced flow*, Composite Structures, September 1995, 32(1-4), 519-529. DOI: 10.1016/0263-8223(95)00025-9.
- J Summerscales, N R L Pearce, P Russell and F J Guild (2001), *Voronoi cells, fractal dimensions and fibre composites*, Journal of Microscopy, February 2001, **201(2)**, 153-162. DOI: 10.1046/j.1365-2818.2001.00841.x.
- J Summerscales, PM Russell, S Lomov, I Verpoest and RS Parnas (2004), The fractal dimension of X-ray tomographic sections of a woven composite, Advanced Composite Letters, 2004, 13(2), 113-121.
- J Summerscales, W Hall and AS Virk (2011), *A fibre diameter distribution factor (FDDF) for natural fibre composites*, Journal of Materials Science, September 2011, **46(17)**, 5876-5880. DOI: 10.1007/s10853-011-5569-6.
- N Vernet, E Ruiz, S Advani, J B Alms, M Aubert, M Barburski, B Barari, J M Beraud, D C Berg, N Correia, M Danzi, T Delavière, M Dickert, C Di Fratta, A Endruweit, P Ermanni, G Francucci, JA Garcia, A George, C Hahn, F Klunker, S V Lomov, A Long, B Louis, J Maldonado, R Meier, V Michaud, H Perrin, K Pillai, E Rodriguez, F Trochu, S Verheyden, M Wietgrefe, W Xiong, S Zaremba, G Ziegmann (2014), *Experimental determination of the permeability of engineering textiles: Benchmark II*, Composites Part A: Applied Science and Manufacturing, June 2014, **61**, 172-184. DOI: 10.1016/j.compositesa.2014.02.010.
- A S Virk, W Hall and J Summerscales (2012), *Modulus and strength prediction for natural fibre composites*, Materials Science and Technology, 2012, **28(7)**, 864-871. DOI: 10.1179/1743284712Y.0000000022.
- G Voronoi (1907), *Nouvelles applications des paramètres continus à la théorie des formes quadratiques*,

Journal für die Reine und Angewandte Mathematik, 1907, **133**, 97-178.
- Y Wang and S M Grove (2009), Continuum dual-scale modelling of Liquid Composite Moulding processes, Journal of Reinforced Plastics and Composites, 2009, 28(12), 1469-1484. DOI: 10.1177/0731684408089533.
- Y Wang, M Motamedi and S M Grove (2008), Modelling microscopic flow in woven fabric reinforcements and its application in dual-scale resin infusion modelling, Composites Part A: Applied Science and Manufacturing, May 2008, 39(5), 843–855. DOI: 10.1016/j.compositesa.2008.01.014
- E W Weisstein (2015), *Voronoi Diagram*, MathWorld - A Wolfram Web Resource: http://mathworld.wolfram.com/VoronoiDiagram.html, accessed 07 November 2015.
- C D Williams, J Summerscales and S M Grove (1996), Resin infusion under flexible tooling (RIFT): a review, Composites Part A: Applied Science and Manufacturing, July 1996, 27A(7), 517-524. DOI: 10.1016/1359-835X(96)00008-5
- C M Worrall and G M Wells (1996), Fibre distribution in discontinuous fibre reinforced plastics: characterisation and effect on materials performance, Proceedings of the 7th European Conference on Composite Materials (ECCM-7), London, 14-16 May 1996, pp. 247-252..

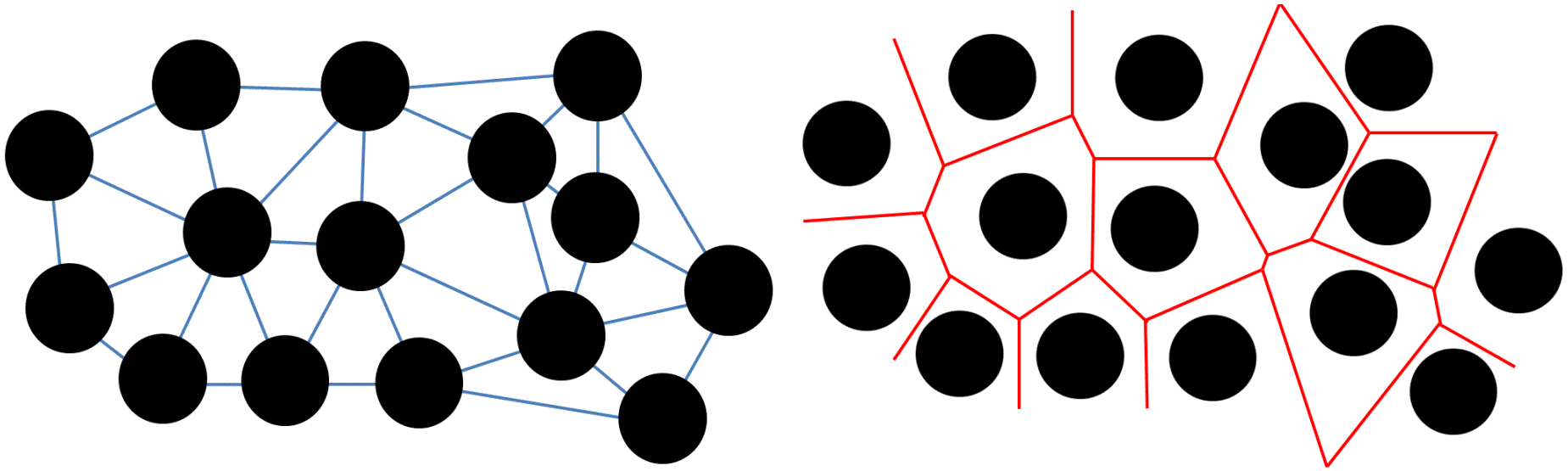

**Figure 1: Delauney (left) and Voronoi (right) tessellations of a set of points**

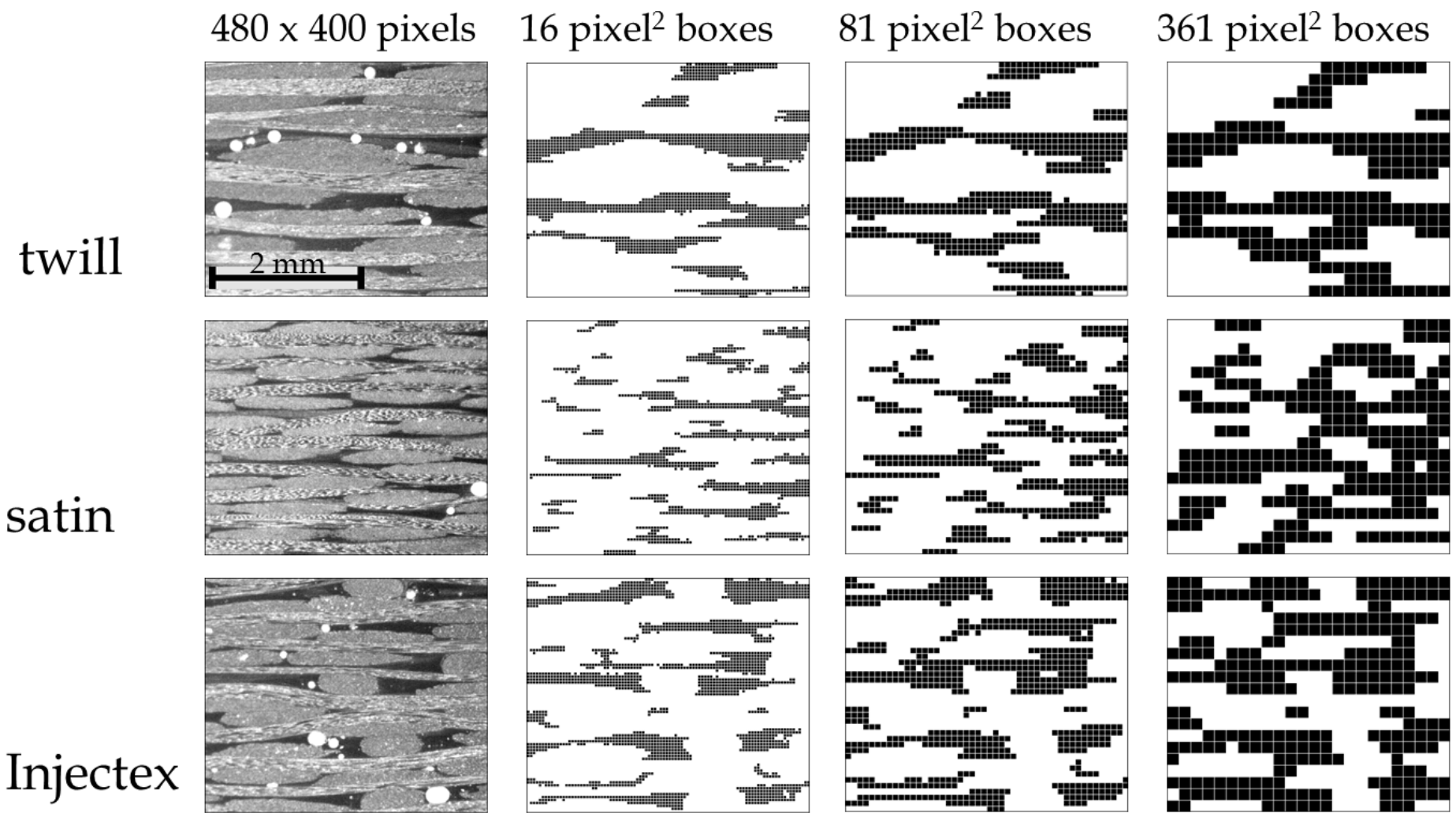


**Figure 2: Representative images showing selected stages of fractal data generation for the resin/void volume fraction.**

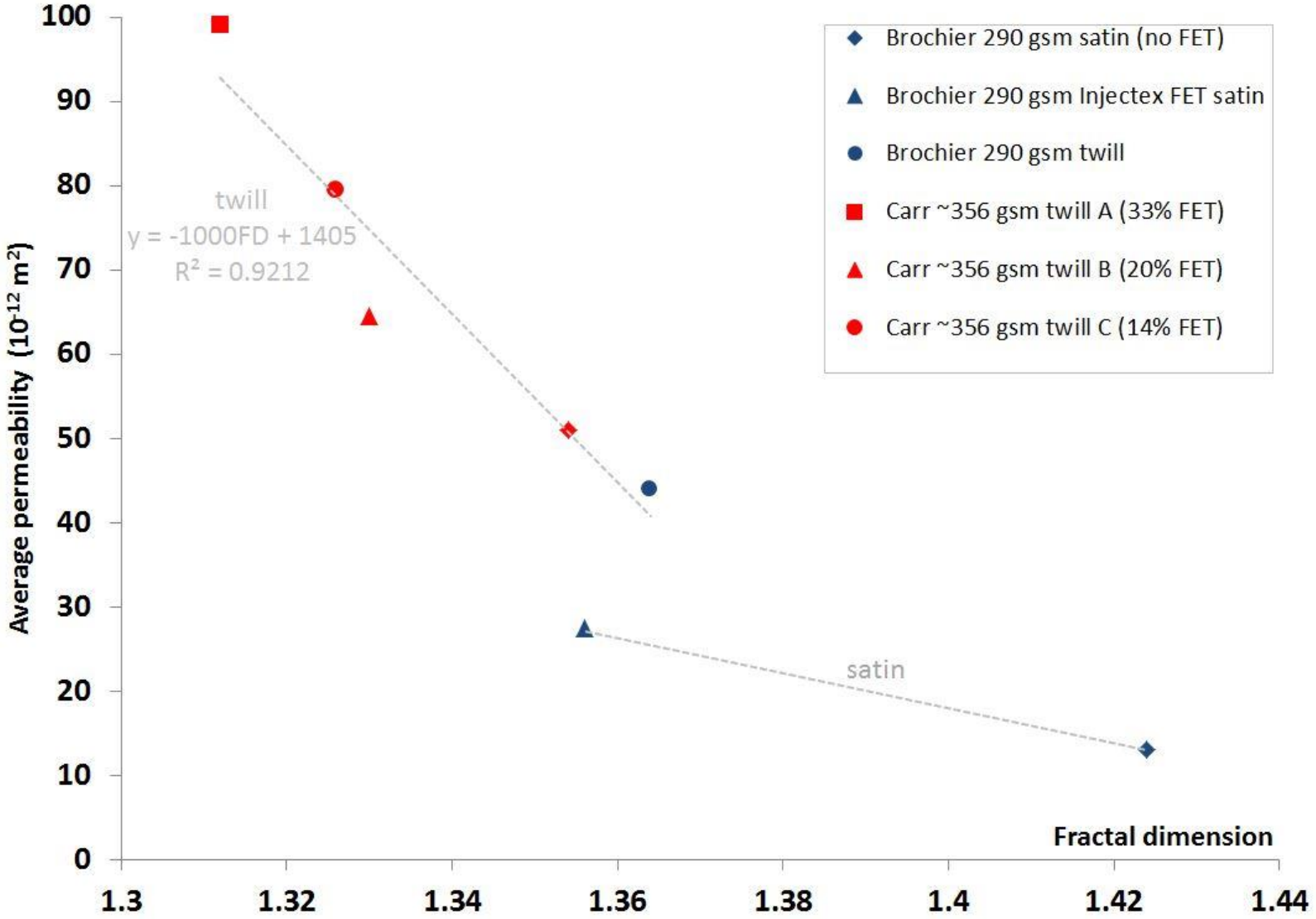


**Figure 3: Permeability plotted against fractal dimension (from resin) for Brochier and Carr Reinforcements fabrics**

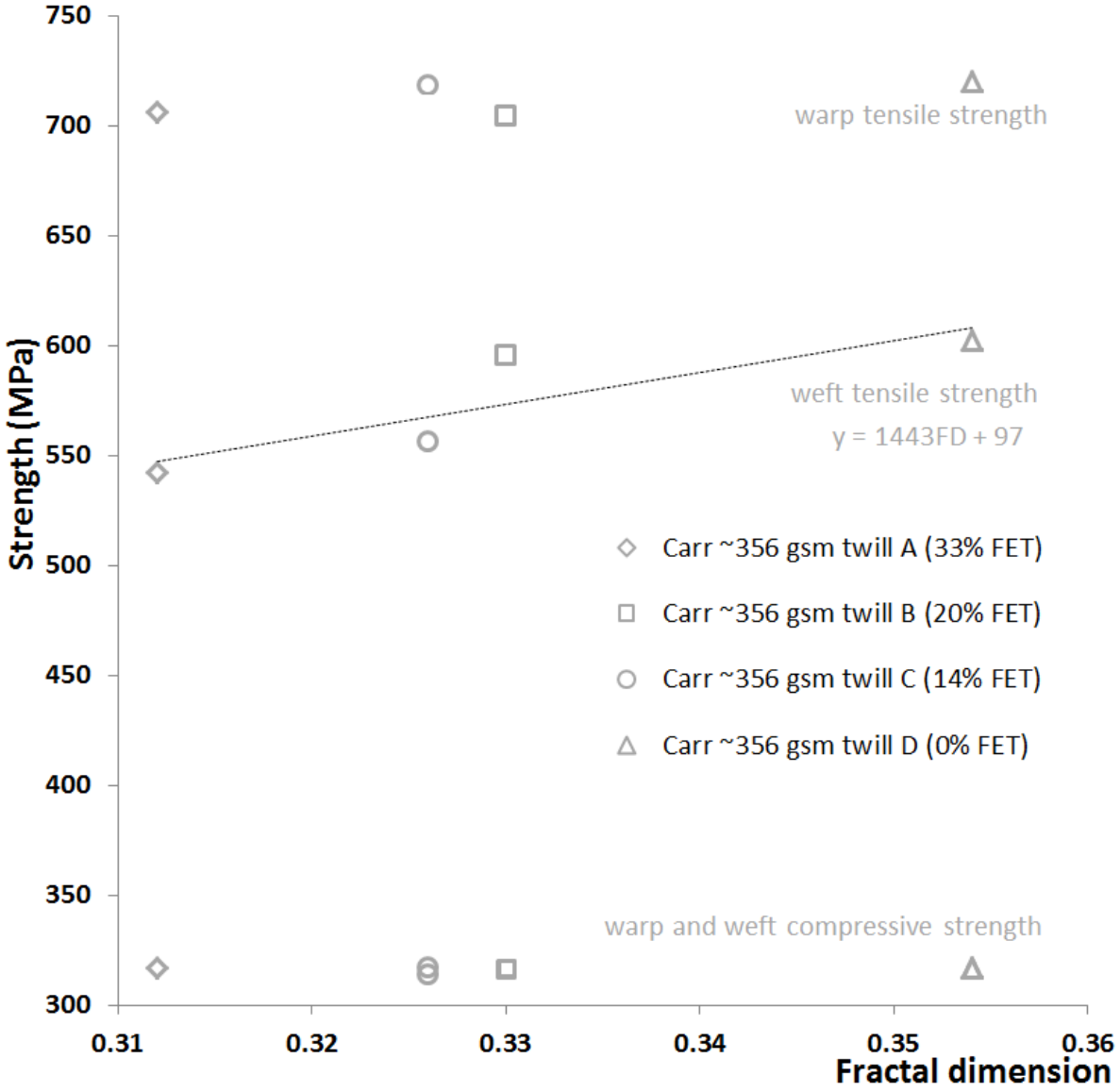


**Figure 4: Tensile and compressive strengths for Carr twill fabrics with differing proportions of flow-enhancing tows. Warp tensile and compressive and weft compressive strengths sensibly constant but weft tensile strength rises with fractal dimension (not with fibre volume fraction).**